
Figures and figure supplements

Identification of a weight loss-associated causal eQTL in *MTIF3* and the effects of *MTIF3* deficiency on human adipocyte function

Mi Huang et al.

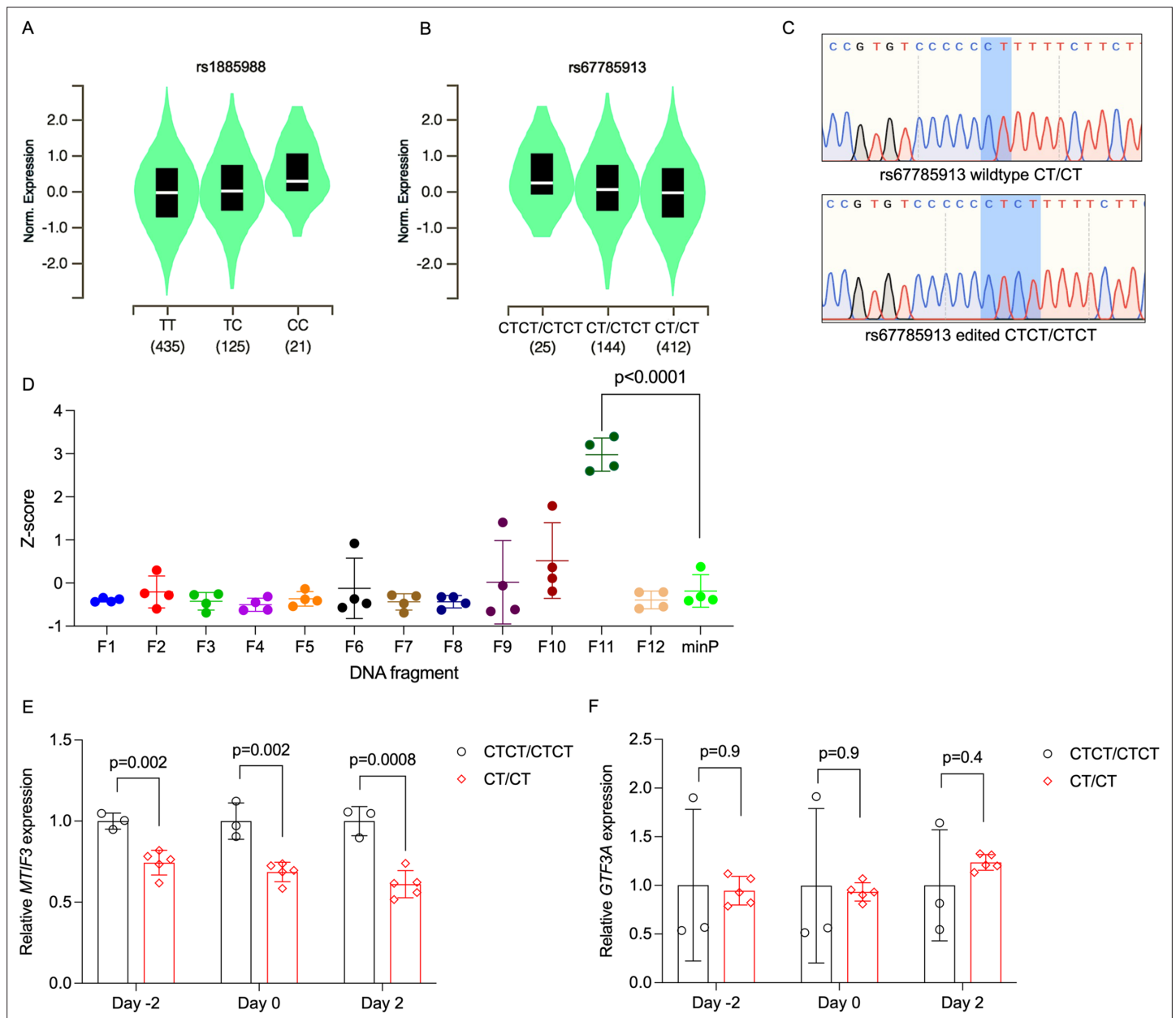


Figure 1. Identification of rs67785913 as a causal cis-eQTL for *MTIF3*. **(A)** Violin plot of *MTIF3* expression in subcutaneous adipose tissue for rs1885988 from Genotype-Tissue Expression (GTEx) Project eQTL. **(B)** Same as in **(A)**, but for rs67785913. **(C)** Representative Sanger sequencing traces of rs67785913 CTCT/CTCT and CT/CT clones obtained after CRISPR/Cas9-mediated allele editing and single-cell cloning. **(D)** Normalized Z-score plot of luciferase reporter assays using vectors carrying different DNA fragments of the *MTIF3* gene cloned into pGL4.23 luciferase reporter vector. Hypothesis testing was performed by comparing the transcriptional enhancer activity of each of the 12 vectors (F1–12) to the empty vector (minP). All data were plotted as mean \pm standard deviation (SD), $n = 4$ independent experiments, p values are presented in each graph; ordinary one-way analysis of variance (ANOVA) was used for statistical analysis. **(E)** Relative *MTIF3* expression (mRNA) in rs67785913 allele-edited cells 2 days before, at, or 2 days post-differentiation induction (day -2, 0, and 2, respectively). $n = 3$ clonal populations for CTCT/CTCT genotype, $n = 5$ clonal populations for CT/CT genotype, error bars show SD. **(F)** as in **(E)**, but for *GTF3A* (mRNA) expression. Two-tailed Student's t-test was used; p values are presented in each graph.

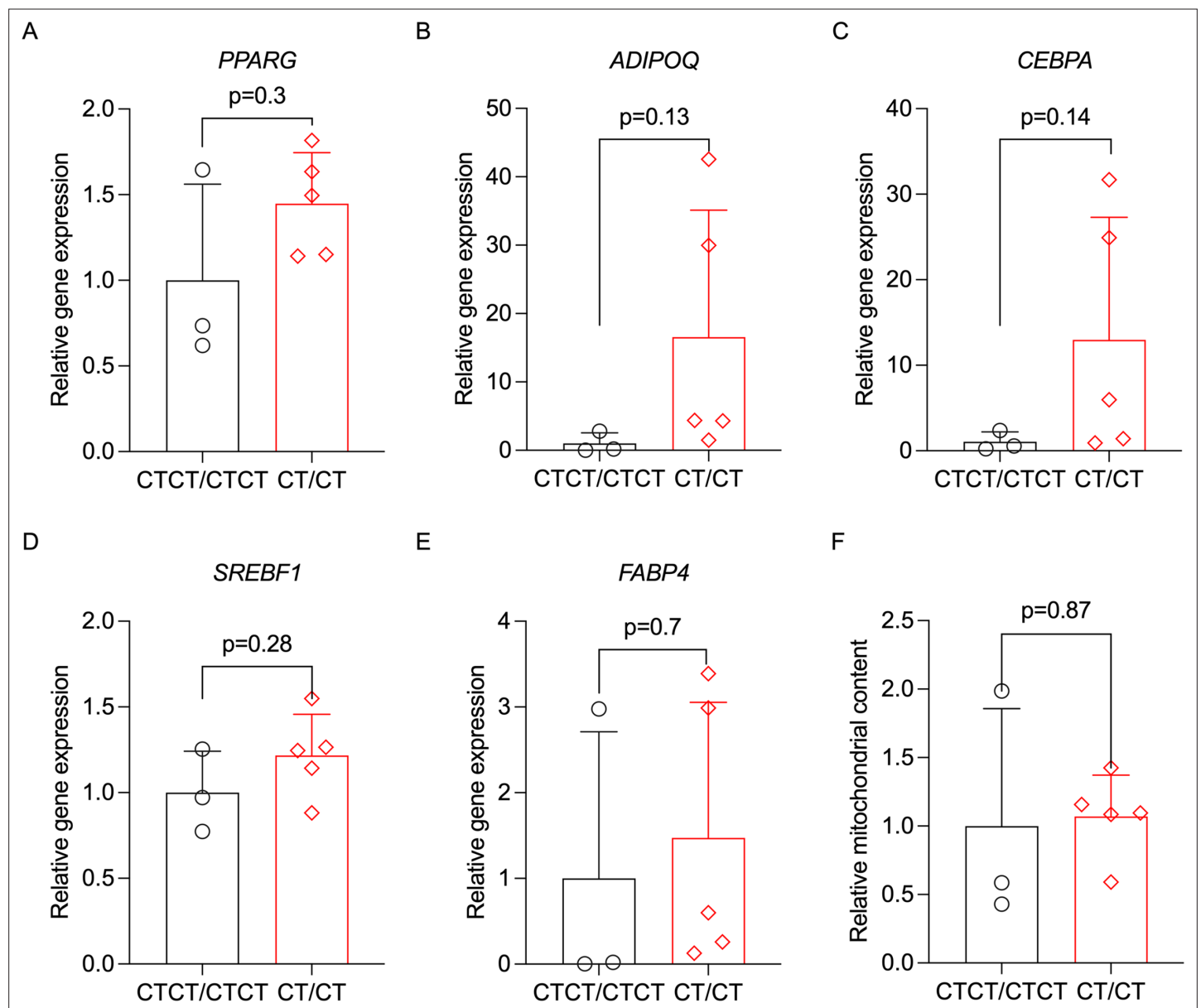


Figure 1—figure supplement 1. To test if rs67785913 affects adipogenic differentiation in hWAs cells, we differentiated the rs67785913 allele-edited cells (CTCT/CTCT vs. CT/CT) for 12 days. We then used qPCR to quantify adipogenesis marker gene expression and mitochondrial content (mtDNA). Neither *PPARG*, *ADIPOQ*, *CEBPA*, *SREBF1*, and *FABP4* gene expression (panels A–E) or mitochondrial content (panel F) were significantly different between the two rs67785913 genotypes. $n = 3$ clonal cell lines with CTCT/CTCT genotype, $n = 5$ clonal cell lines for CT/CT genotype. Error bars show standard deviation. Statistical analyses were performed using paired Student's t-test, and p values are presented in the graphs.

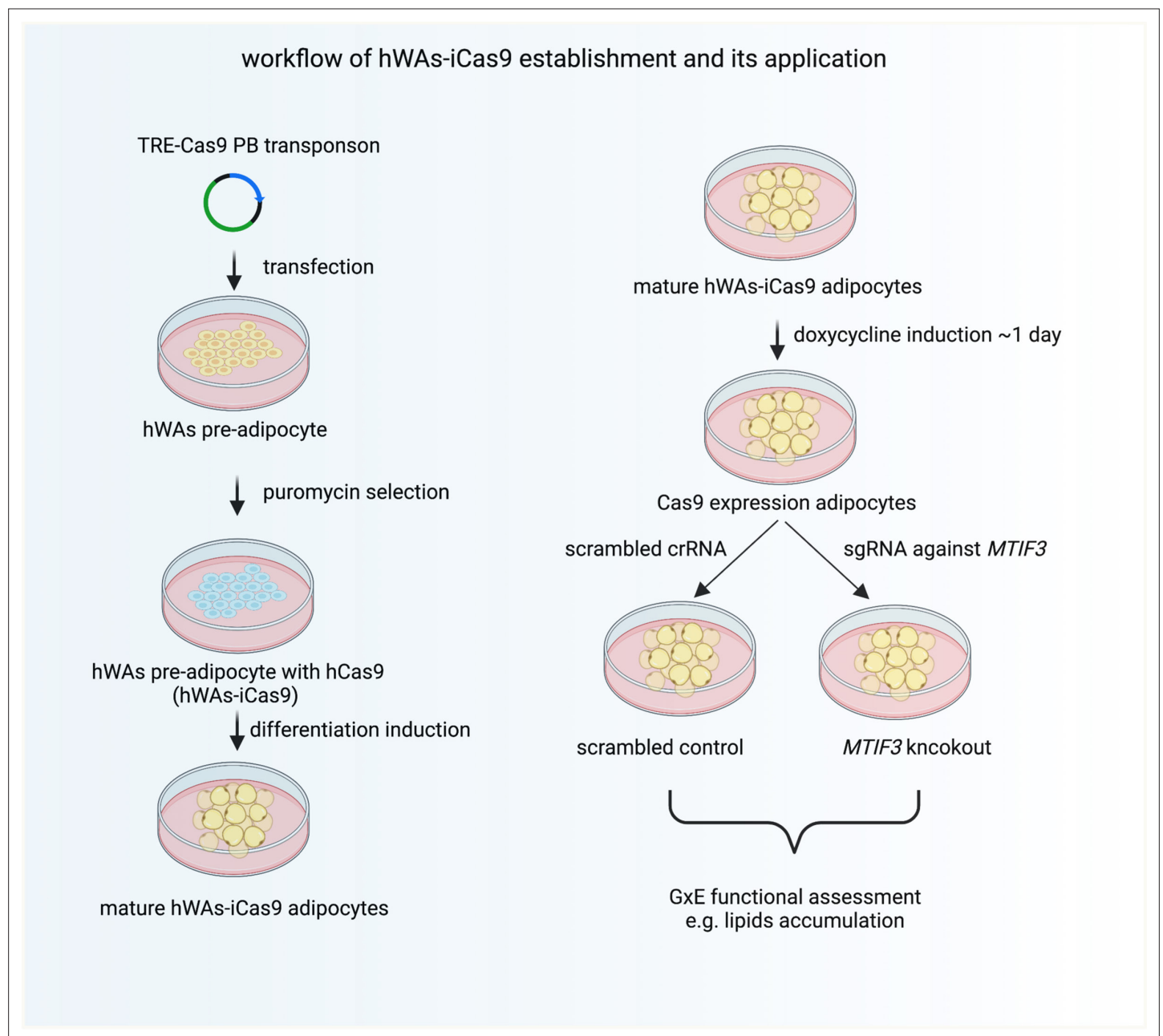


Figure 2. The workflow of establishing hWAs-iCas9 cell line and its application in studying *MTIF3* and environment interactions in vitro.

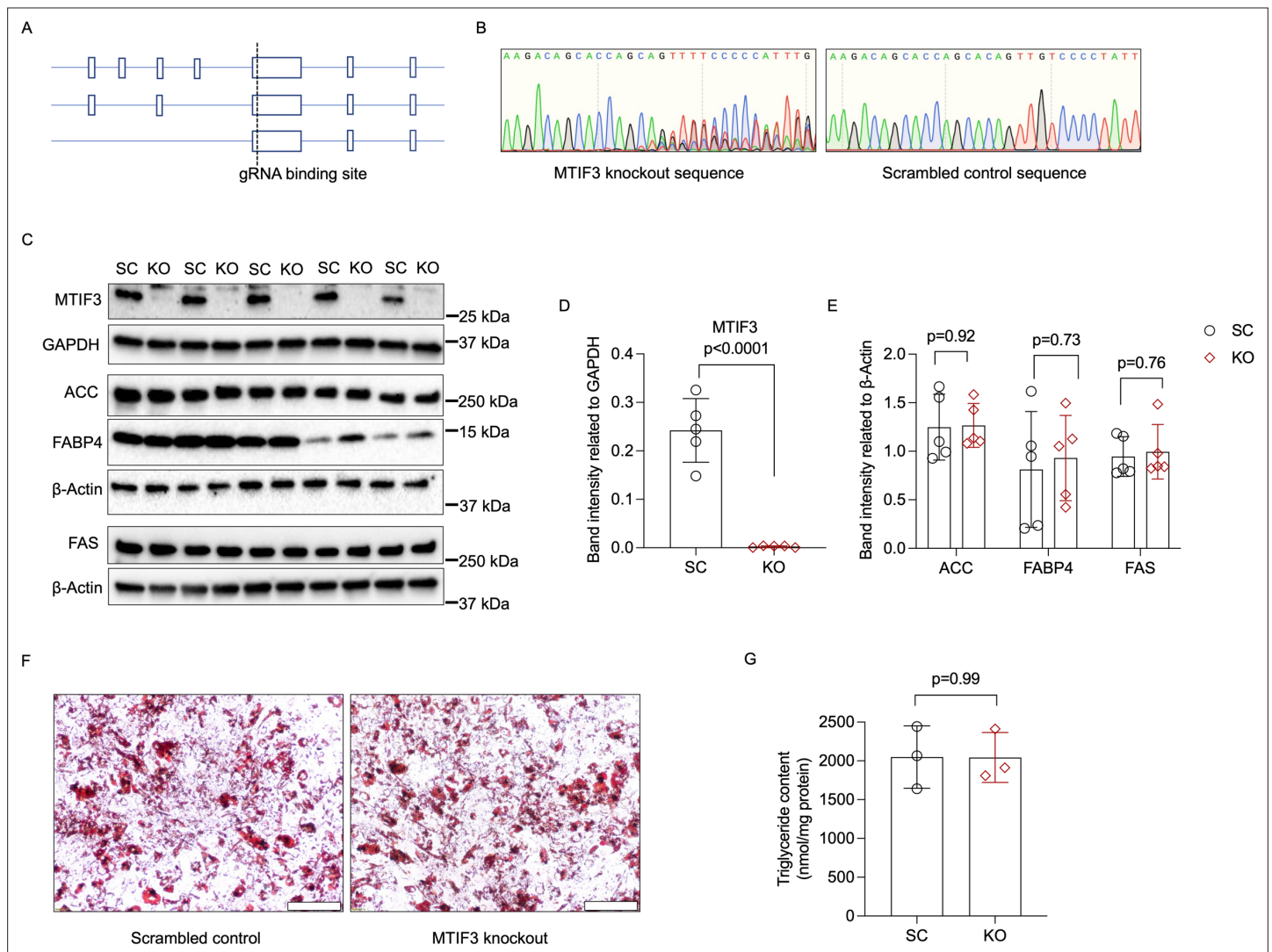


Figure 3. *MTIF3* perturbation in mature adipocytes does not affect adipocyte-specific protein expression or total triglyceride content. **(A)** An illustration of Cas9-specific single guide RNA (sgRNA)-binding site in the exon expressed in all three *MTIF3* protein-encoding transcripts. **(B)** Representative Sanger sequencing of control and knockout hWAs mature adipocytes. **(C)** Immunoblots of adipocyte markers in scrambled control and *MTIF3* knockout adipocytes, $n = 5$ independent experiments. **(D)** Quantitative analysis of *MTIF3* band densities in (C). **(E)** Quantitative analysis of ACC, FABP4, and FAS band densities in (C). **(F)** Representative Oil-red O staining images of control and *MTIF3* knockout in hWAs mature adipocytes. Scale bar is 200 μm. **(G)** Total triglyceride content in scrambled control (SC) and *MTIF3* knockout (KO) cells. $n = 3$ independent experiments. Error bars show standard deviation in all plots. Statistical analysis was performed using two-tailed Student's *t*-test, *p* values are presented in each graph. Uncropped blot images for (C) and raw.scn data files can be found in **Figure 3—source data 1**.

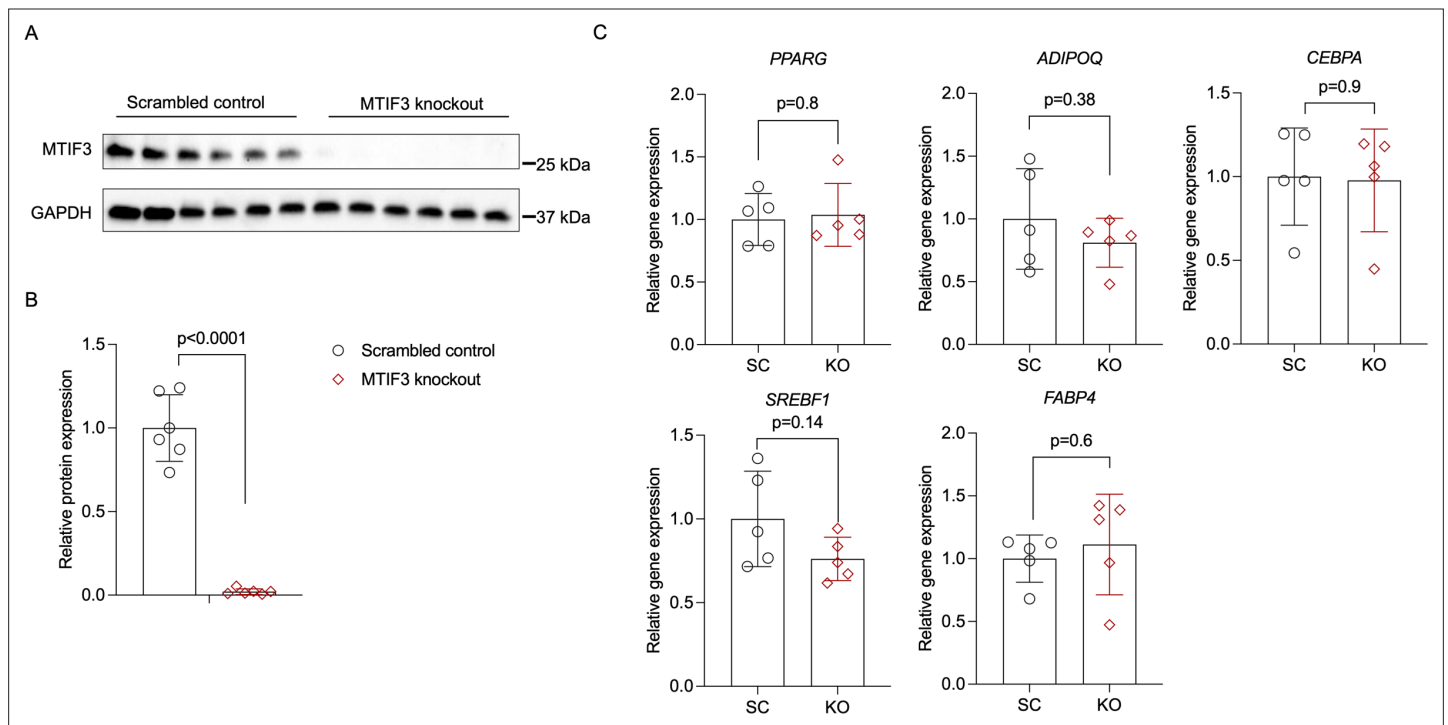


Figure 3—figure supplement 1. To test the effects of *MTIF3* knockout on adipogenic differentiation in hWAs-iCas9 cell line, we first induced *MTIF3* knockout in hWAs-iCas9 pre-adipocytes, then differentiated them using standard adipogenic differentiation cocktail. After 12 days of differentiation, we assessed *MTIF3* knockout efficiency using western blots, and examined adipogenic marker gene expression by RT-qPCR. *MTIF3* expression was efficiently decreased in the knockout cells in $n = 6$ independent experiments (panels **A**, **B**). There were no significant differences between scrambled control and *MTIF3* knockout cells on adipogenesis markers *PPARG*, *ADIPOQ*, *CEBPA*, *SREBF1*, and *FABP4* expression (panel **C**); $n = 5$ independent experiments. Error bars show standard deviation. Statistical analyses were performed using paired Student's *t*-test, and *p* values are presented in the graphs. Uncropped blot images for panel A and raw.scn data files can be found in **Figure 3—figure supplement 1—source data 1**.

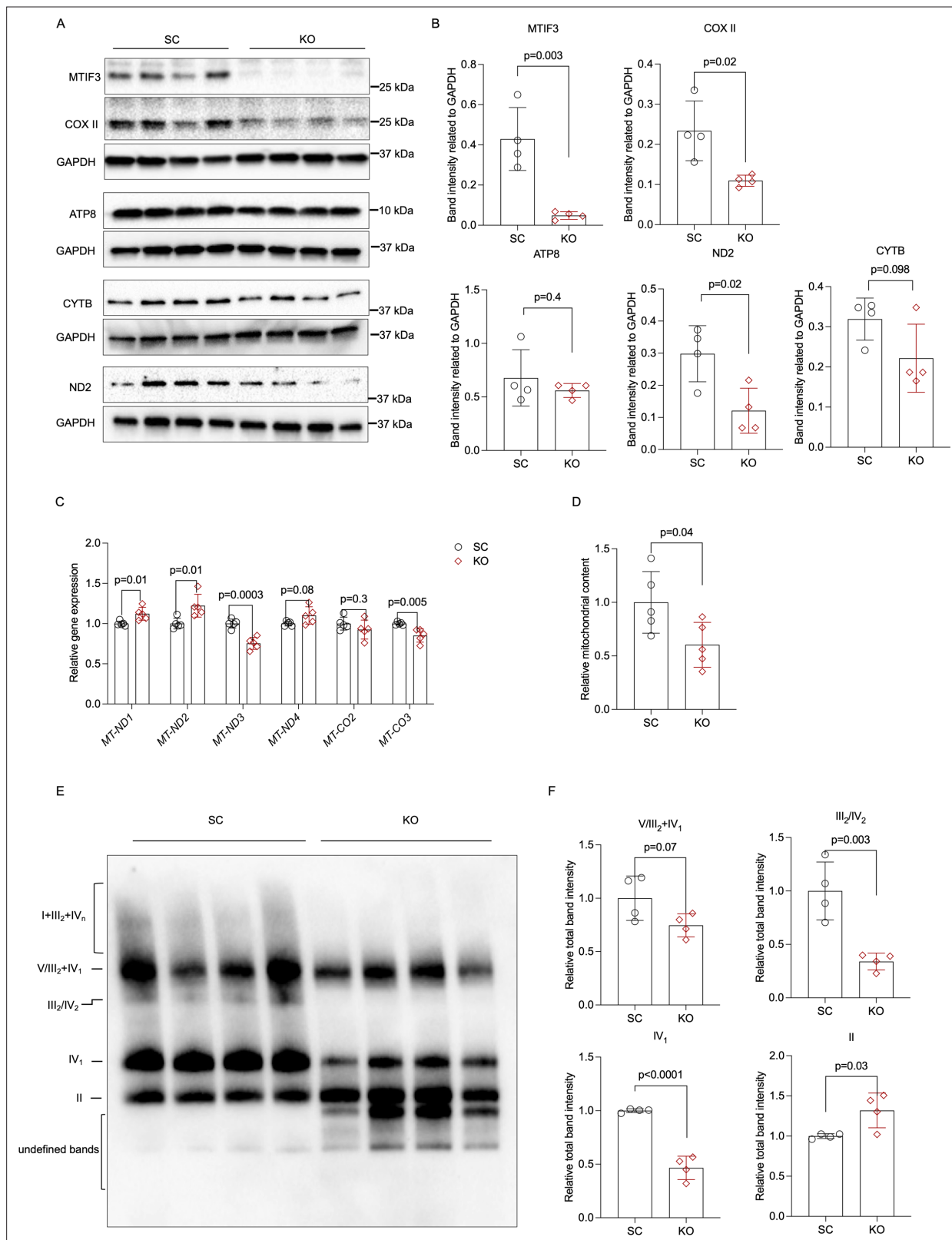


Figure 4. MTIF3 perturbation in mature adipocytes disrupts mitochondrial gene expression and OXPHOS complex assembly. **(A)** Immunoblots of mitochondrial genome-encoded proteins in scrambled control and *MTIF3* knockout adipocytes. **(B)** Quantitative analysis of band densities in **(A)**. **(C)** qPCR for mitochondrial gene expression in scrambled control and *MTIF3* knockout adipocytes, $n = 5$ independent experiments. **(D)** Relative mitochondrial DNA content in scrambled control and *MTIF3* knockout adipocytes, $n = 5$ independent experiments. **(E)** Immunoblots of mitochondrial

Figure 4 continued on next page

Figure 4 continued

OXPHOS complex assembly after Blue Native-PAGE electrophoresis, $n = 4$ independent experiments. **(F)** Quantitative analysis of band densities in **(E)**. Error bars show standard deviation in all plots. Statistical analysis was performed using two-tailed Student's *t*-test, *p* values are presented in each graph. Uncropped blot images for **(A)** and raw.scn data files can be found in **Figure 4—source data 1**. Uncropped blot images for **(E)** and raw.scn data files can be found in **Figure 4—source data 2**.

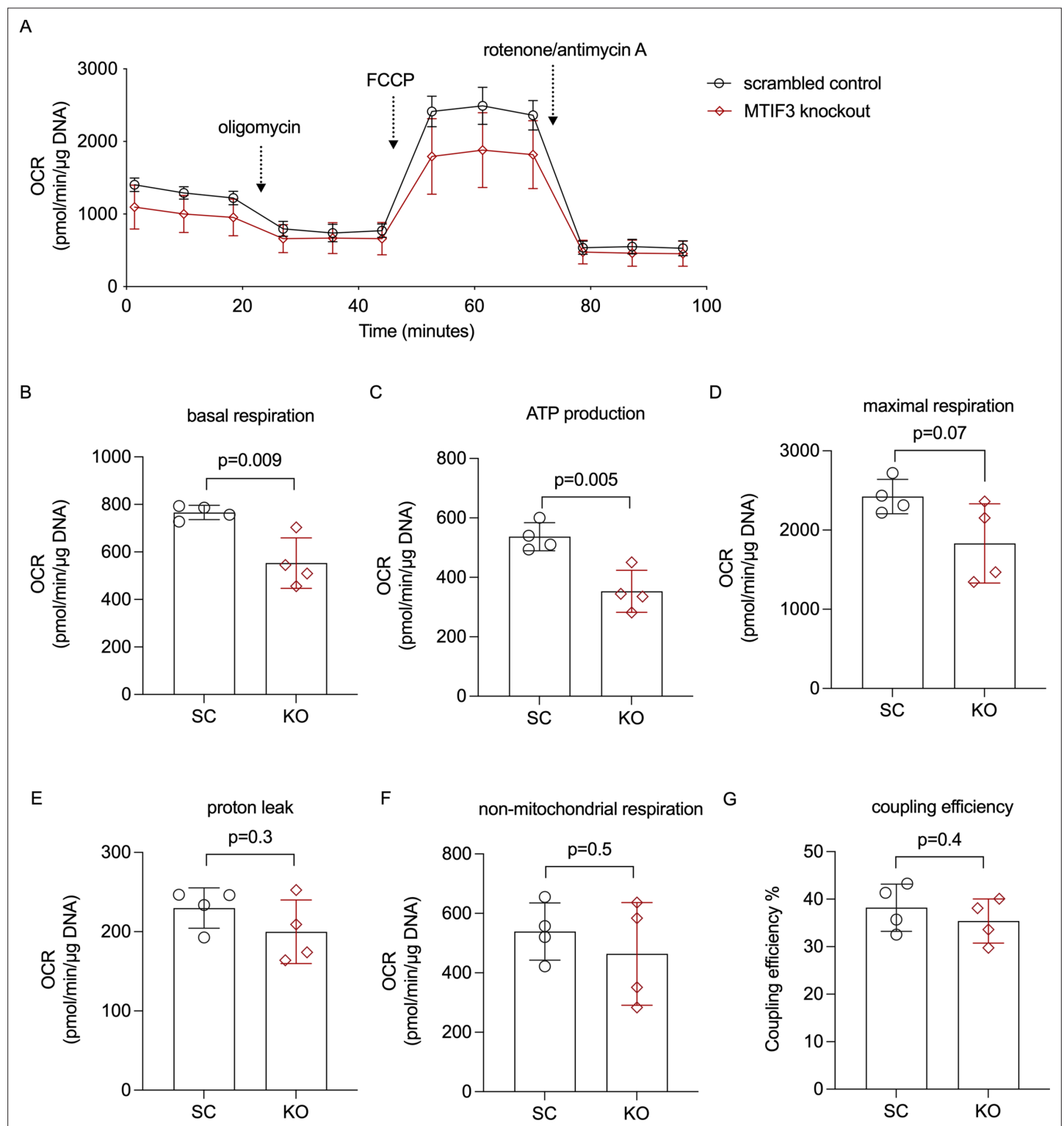


Figure 5. Cellular mitochondrial respiration in hWAs adipocytes. **(A)** The average oxygen consumption rate (OCR) traces during basal respiration, and after addition of oligomycin, FCCP, and rotenone/antimycin A. **(B)** Basal respiration OCR, $n = 4$ different cell passages. **(C)** ATP production OCR, $n = 4$ different cell passages. **(D)** Maximal respiration OCR, $n = 4$ different cell passages. **(E)** Proton leak OCR, $n = 4$ different cell passages. **(F)** Non-mitochondrial respiration OCR, $n = 4$ different cell passages. **(G)** Coupling efficiency, $n = 4$ different cell passages. Error bars show standard deviation. Statistical analyses were performed using paired Student's *t*-test in each condition, *p* values are presented in each graph.

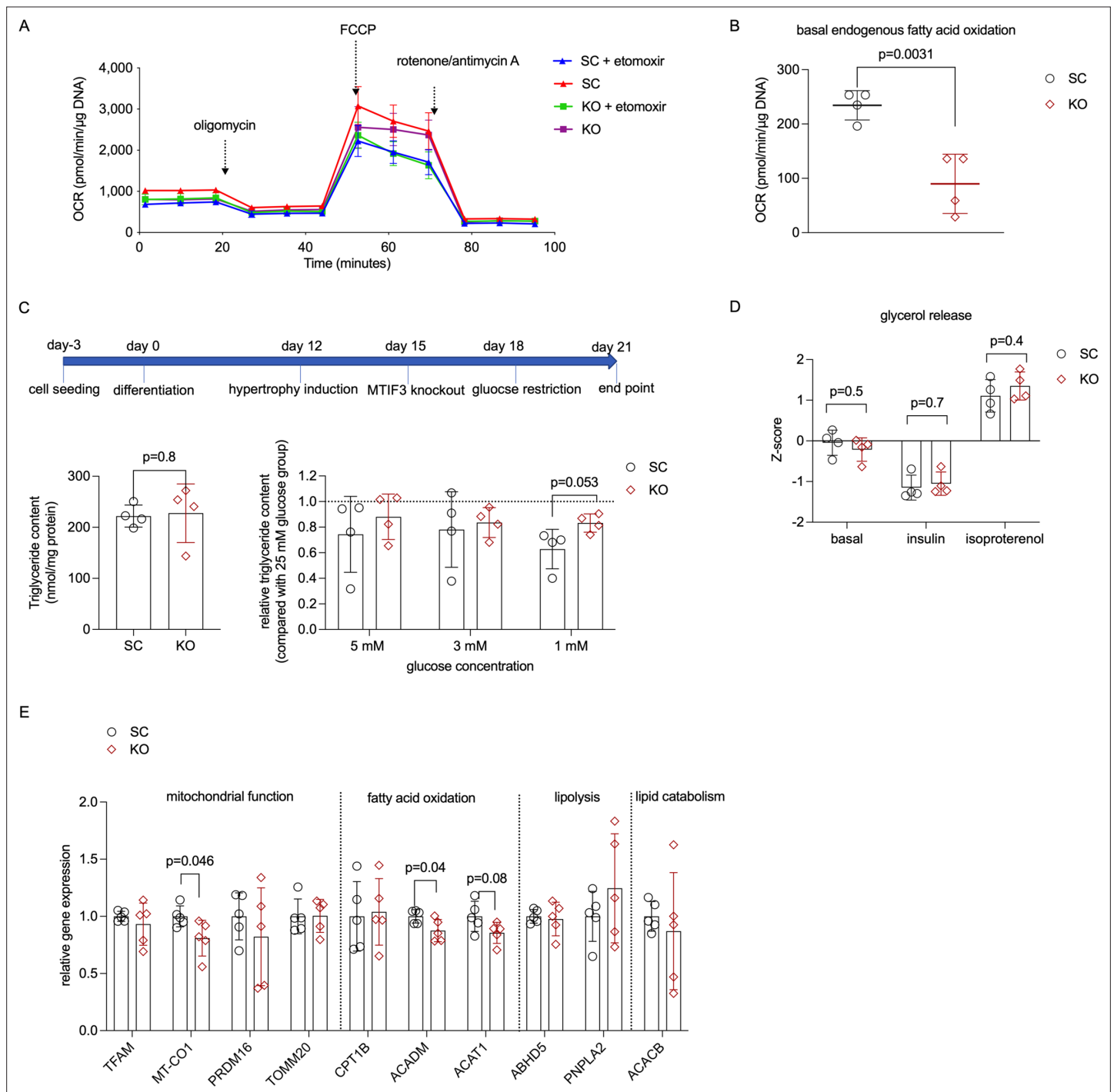


Figure 6. *MTIF3* perturbation affects adipocyte fatty acid oxidation. **(A)** A representative Seahorse oxygen consumption rate (OCR) trace for endogenous fatty acid oxidation assay. *MTIF3* knockout and scrambled control adipocytes were treated with or without etomoxir for 15 min before the assay. Following the basal OCR measurement, oligomycin, FCCP (carbonyl cyanide-*p*-trifluoromethoxyphenylhydrazine), and rotenone + antimycin A were added sequentially to measure the detection of ATP production OCR, maximal respiration OCR and non-mitochondrial respiration OCR. **(B)** Basal endogenous fatty acid oxidation OCR in scrambled control (SC) and *MTIF3* knockout (KO) adipocytes, $n = 4$ independent experiments. **(C)** Upper panel: workflow of glucose restriction in differentiated adipocytes; Lower left panel: total triglyceride content in scrambled control (SC) and *MTIF3* knockout (KO) adipocytes in 25 mM glucose conditions; Lower right panel: triglyceride content in adipocytes cultured in glucose-restricted conditions (5, 3, and 1 mM) relative to adipocytes cultured in 25 mM glucose, $n = 4$ independent experiments. **(D)** Z-score-normalized data for glycerol release in scrambled control and *MTIF3* knockout adipocytes under basal, insulin-stimulated, and isoproterenol-stimulated conditions, $n = 4$ independent experiments. **(E)** qPCR for mitochondrial and adipocyte-related gene expression in scrambled control and *MTIF3* knockout adipocytes. Error bars show standard deviation in all plots. Statistical analysis was performed using two-tailed Student's *t*-test, *p* values are presented in each graph.

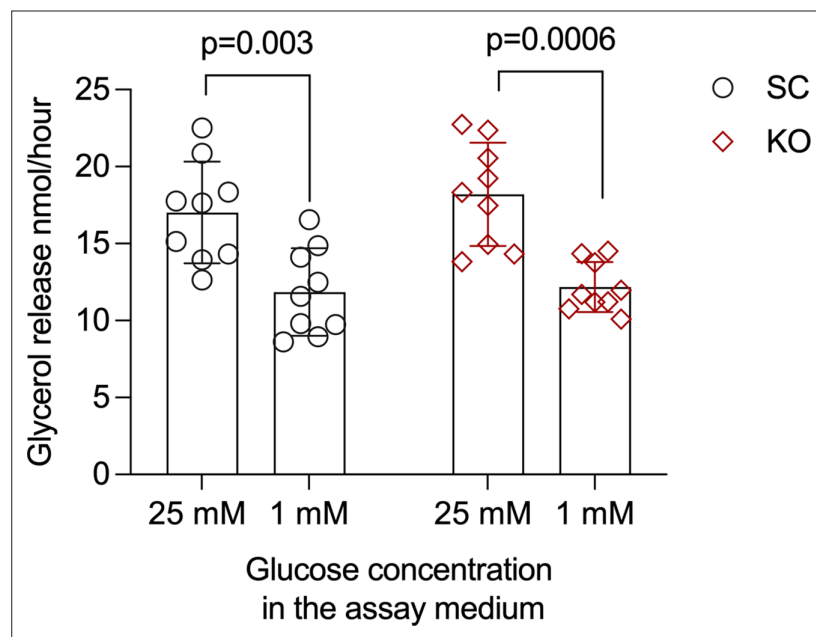


Figure 6—figure supplement 1. *MTIF3* knockout does not affect mature adipocyte glycerol release at either 25 or 1 mM glucose condition. To assay this, we incubated the differentiated adipocytes in glycerol release assay medium supplemented with either 25 or 1 mM glucose. We then determined glycerol content in each sample after 2-hr incubation. We found no differences in glycerol release between scrambled control and *MTIF3* knockout cells cultured in the same glucose concentration. Notably, both scrambled control and *MTIF3* knockout cells had significantly decreased glycerol release in 1 mM glucose restriction condition. $n = 3$ independent experiments, with 3 replicates per group and experiment. Error bars show standard deviation. Statistical analyses were performed using paired Student's *t*-test, and *p* values are presented in the graph.

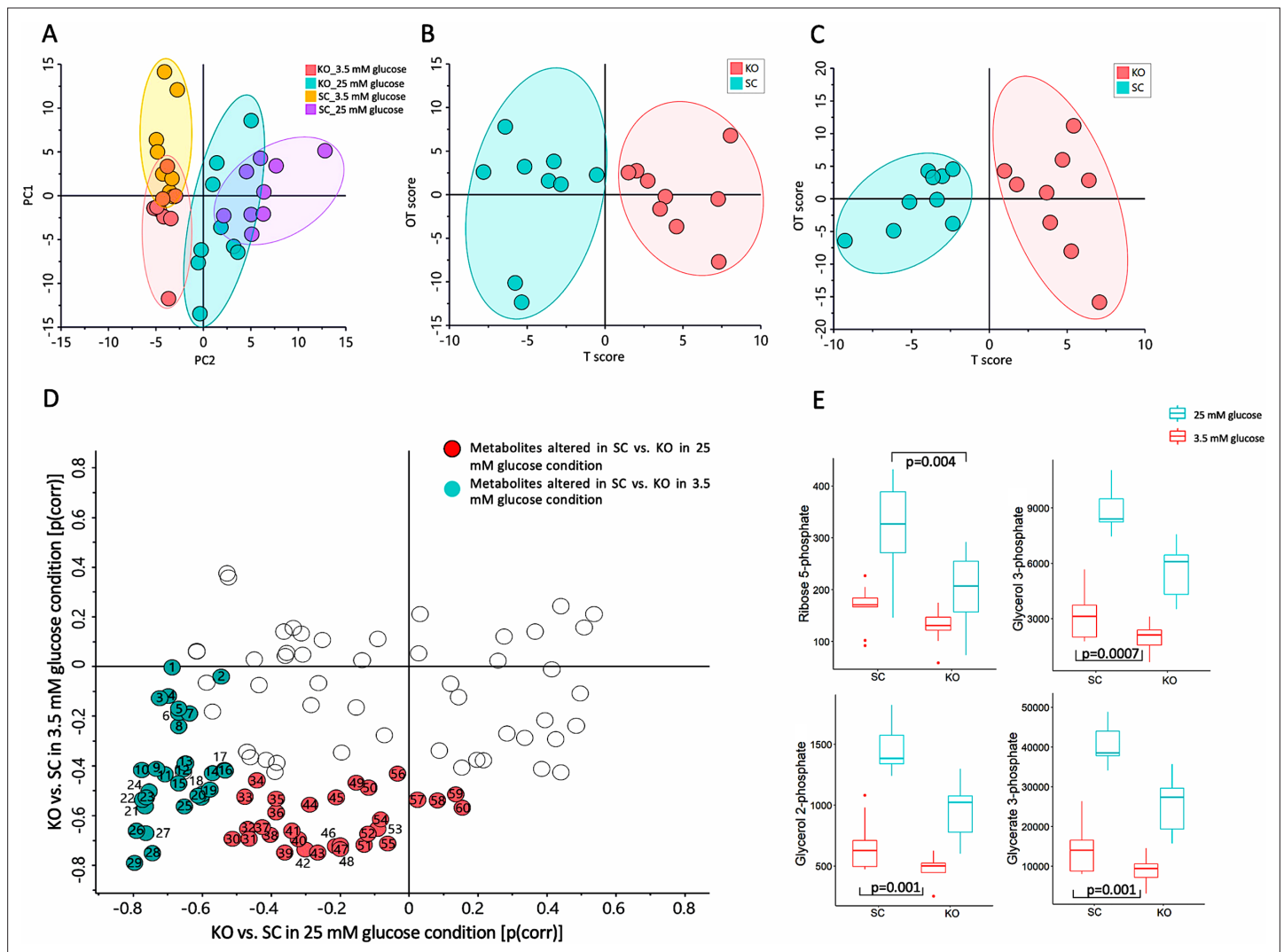


Figure 7. Mass spectrometry-based metabolomics data for control (SC) and *MTIF3* knockout (KO) cells in 25 mM glucose (NF, normal feeding) and 5 mM glucose (GR, glucose-restricted) conditions. (A) Principal component analysis (PCA) score plot displaying the discrimination between *MTIF3* knockout and control cells in normal and glucose-restricted conditions (PC1: 28%, PC2: 19%). (B) Orthogonal projections to latent structures discriminant analysis (OPLS-DA) score plot showing classification of *MTIF3* knockout and control cells in 25 mM glucose condition. (C) OPLS-DA score plots showing classification of *MTIF3* knockout and control cells in glucose-restricted condition. (D) Shared and unique structures (SUS) plot, based on OPLS-DA models in (B, C), showing glucose concentration-dependent differences between *MTIF3* knockout and control cells. (E) Box plots showing the abundance of some of the significantly altered metabolites in normal and *MTIF3* knockout cells in normal and glucose-restricted conditions. Statistical analysis was performed using two-way analysis of variance (ANOVA) test, p values are presented in each graph.